

Effects of Post-sintering Annealing on (NdLa)-(FeCo)-B Magnets

Wei Tang*^{1,2}, Jing Wang^{1,2}, Chaochao Pan², Kinjal Gandha⁵, Ikenna C. Nlebedim^{2,4}, Ryan Ott^{1,2},
and Jun Cui^{1,2,3}

¹ Division of Materials Science and Engineering, Ames National Laboratory, Ames, IA 50011, USA

² Division of Critical Materials, Critical Materials Innovation Hub, Ames National Laboratory, Ames, IA 50011, USA

³ Department of Materials Science and Engineering, Iowa State University, Ames, IA 50011, US

⁴ Department of Electrical and Computer Engineering, Iowa State University, Ames, IA 50011, USA

⁵ MP Materials Corporation, 1301 Solana Blvd #1545, Westlake, TX76262, USA

*Corresponding author: Wei Tang, Email: weitang@ameslab.gov

Abstract

A common limitation of La substitutions into (Nd, La)₂Fe₁₄B magnet is the reduction of the anisotropy field (H_a), which decreases magnet's coercivity (H_{cj}). Adding a small amount of Pr-Cu to the La-containing Neo magnet may modify the grain boundary (GB), which can help recover a fraction of the degraded H_{cj} . An optimal GB modification requires a carefully designed post-sinter heat treatment, which is the focus of this work characterizing the effects of multi-step post-sintering annealing on the evolutions of microstructure and magnetic properties. We find that Nd and Cu concentrations at GB and triple junction (TJ) increase when the annealing temperatures are lowered. Annealing temperatures of 580 and 480 °C (near RE-rich eutectic temperatures) enabled the development of a thick and continuous GB phase, which helps to magnetically decouple the grains, and thus, enhance H_{cj} . For the alloy with 25% Nd replaced by La and with the addition of 7.5 wt.% of Pr₆₈Cu₃₂ as GB modifier, the optimized multi-step post-sinter annealing improved the H_{cj} from 4.8 kOe to 9 kOe.

I. INTRODUCTION

Neo permanent magnets are widely used in EV traction-drive motors and wind turbine generators due to their high maximum energy product $(BH)_{\max}$.^{1,2} Neo magnets with $(BH)_{\max}$ ranging from 35 to 52 MGOe are mass-produced and used in numerous technologies. As the world is pursuing more energy efficiency and renewable energy applications, the annual demand for Neo magnets is expected to double from 190,000 tons in 2020 to 450,000 tons in 2030.³ Consequently, the supply risk of the key rare earth (RE) elements used in the Neo magnet, such as Nd, Pr, and Dy, has become a serious concern. In contrast, La and Ce are generally overly produced, however, they tend to deteriorate the hard magnetic properties of Neo magnets. According to the U.S. Bureau of Mines, the ore from Mountain Pass in California contains about 33.20% La_2O_3 , 49.10% CeO_2 , 4.34% Pr_6O_{11} , 12.00% Nd_2O_3 and 0.03% of Dy_2O_3 .⁴ When mining the critical elements Nd and Pr, a large amount of La and Ce oxides is produced as byproducts. With the Ce and La oxides being sold at a fraction of the prices of the Nd and Pr oxides. Therefore, if La and Ce can be partially substituted for Nd and Pr in Neo magnets without severe degradation of the hard magnetic properties, the overall economics of the mining and magnet-making operation could be improved.

Table I shows the magnetization, anisotropy field and Curie temperatures of various 2:14:1 type RE compounds. The anisotropy fields of the $\text{La}_2\text{Fe}_{14}\text{B}$ ($H_a = 20$ kOe) and $\text{Ce}_2\text{Fe}_{14}\text{B}$ ($H_a = 26$ kOe) compounds are significantly lower than that of $\text{Nd}_2\text{Fe}_{14}\text{B}$ ($H_a = 73$ kOe). Assuming 20% of these anisotropy fields can be utilized for coercivity, the magnets made of these two compounds will have a coercivity H_{c_j} less than 5.2 kOe at room temperature.

Table I. Saturation magnetization M_s , anisotropy field H_a , and Curie temperatures T_c of various 2-14-1 type RE compounds at room temperature.⁵

Compound	La ₂ Fe ₁₄ B	Ce ₂ Fe ₁₄ B	Nd ₂ Fe ₁₄ B	Pr ₂ Fe ₁₄ B	Dy ₂ Fe ₁₄ B
M _s (kG)	13.8	11.7	16.0	15.6	7.1
H _a (kOe)	20	26	73	75	150
T _c (K)	530	424	585	565	598

Li et al. studied the effect of La substitution on the intrinsic magnetic properties and microstructure of (Nd_{1-x}La_x)₃₀Fe₆₉B magnets.⁶ They showed that with La increasing from x = 0 to 0.6, the H_a decreased from 65 to 47 kOe, and the saturation magnetization (M_s) decreased from 15.9 to 13.7 kG. This finding is encouraging, however, the La₂Fe₁₄B compound is not stable at the typical sintering temperatures, which causes phase decomposition and precipitation of soft iron phases.^{7,8,9} The phase instability can be attributed to the large atomic radius of La, compared to other RE elements, which leads to limited solubility in the Nd₂Fe₁₄B phase. In addition, the solubility of La in the Nd₂Fe₁₄B also depends on temperature. The solubility of La decreases at high temperatures. The magnetic properties of La-containing Neo magnets, especially the H_{cj}, generally deteriorate with increasing La content.^{10,11,12} This trend is also applicable for Ce-containing Neo magnets. Currently, the limit of the La and Ce substitution for Nd is about 25 at.%. The 2-14-1 based magnets with La:Nd = 25:75 and Ce:Nd = 25:75 may exhibit H_{cj} of 6.2 and 11.8 kOe, and (BH)_{max} of 35.5 and 39.8 MGOe, respectively.¹⁰

One approach to enhancing the H_{cj} of La/Ce containing Neo magnet is to make the (Nd, Pr)-based 2-14-1 powder and the (La, Ce)-based 2-14-1 powder separately, then mix them together prior to sintering.^{13,14,15} Magnets made by this dual-alloy powder method can be superior to ones synthesized by the single alloy powder approach, i.e., melting the La, Ce, Nd, Pr all together to form the (La, Ce, Nd, Pr)-Fe-B master alloy, then following the rest of the magnet making process. The improved properties of the dual-alloy powder approach were attributed to the heterogeneous REE distributions across the grain boundary (GB).¹⁶ Another approach to retaining coercivity is to

directly modify the GB by diffusing low melting point non-magnetic metals/alloys into the magnet.^{17, 18} The diffusion enables uniform distribution of the non-magnetic GB phase. Alternatively, these GB modifier materials can be first made into powder form, then mixed with the primary powder and then sintering.^{19,20} The high temperature of the sintering process may cause some GB modifying materials to diffuse into the grains, but most remain at the GB. This approach is different from the dual alloy powder approach, albeit both involve mixing two powders.

These GB engineering approaches aim to create a continuous network of non-magnetic materials that will magnetically isolate the grains and cut off the propagation of magnetization reversal, thereby improving coercivity.²¹ Achieving these ideal microstructures with the desired compositions requires a post-sinter annealing process tailored specifically to the GB modifier material.^{22,23,24} In our previous GB engineering studies on Neo magnets, we found the addition of $\text{Pr}_{68}\text{Cu}_{32}$ alloy (at.%) can significantly improve H_c in Nd-based magnets.²⁵ Here, we report the results of heat treatment studies for $(\text{Nd}_{0.75}\text{La}_{0.25})_{2.6}\text{Fe}_{11.9}\text{Co}_2\text{Ga}_{0.1}\text{B}$ sintered magnets with $\text{Pr}_{68}\text{Cu}_{32}$ as the GB modifying material. The effects of the post-sinter annealing process on microstructures, local compositions, and magnetic properties are discussed.

II. EXPERIMENTAL DETAILS

Commercial grade (>99.9 wt% purity) Nd, La, Pr, Fe, Co, Fe-B, Cu, and Ga were used to prepare the master alloy with a nominal composition of $(\text{Nd}_{0.75}\text{La}_{0.25})_{2.6}\text{Fe}_{11.9}\text{Co}_2\text{Ga}_{0.1}\text{B}$. The alloys were first arc-melted, then strip-cast to flakes ($\sim 125 \mu\text{m}$ thickness) with the linear wheel speed set at 1.5 m/s. The flakes were subjected to hydrogen decrepitation process and ground into coarse powders (200-400 μm). The powder of the grain boundary modifier alloy $\text{Pr}_{68}\text{Cu}_{32}$ (mole ratio) was prepared by the arc-melting, melt-spinning, and ball-milling processes. The obtained coarse

Pr-Cu powder ($\sim 75 \mu\text{m}$) was added to the master NdLa-FeCoGa-B powder at a ratio of 7.5 wt.%. The mixture was ball-milled to finer powder ($\sim 3.5 \mu\text{m}$), then aligned with a 9 T pulsed field in a rubber die, and cold isostatic pressed with a hydrostatic pressure of 500 MPa. The obtained green compacts were sintered at 1080 °C for 1.5 hrs in a vacuum furnace. Six samples were cut out from the as-sintered single block magnet (denoted as S1-S6). They were annealed at different temperatures (900 to 440 °C) with various dwelling times (0.5 to 24 h). After each annealing step, the magnetic properties of the sample were measured before proceeding to the next annealing step. The differential scanning calorimeter (DSC) of samples were measured from room temperature to 1250°C using Netzsch STA 449. The heating or cooling rate is 20°C/min. The magnetic properties of the magnets were measured using a closed-loop B-H hysteresisgrapher tracer and a PPMS DynaCool™ system with maximum applied magnetic field of 2 T and 9 T, respectively. Microstructures and compositions of the magnets were examined using an FEI Teneo field-emission scanning electron microscope (FE-SEM) equipped with an Oxford Aztec energy dispersive detector (EDS).

III. RESULTS

When the as-sintered magnet ($\text{Nd}_{0.75}\text{La}_{0.25}\text{Fe}_{11.9}\text{Co}_2\text{Ga}_{0.1}\text{B}$) containing the GB modifier $\text{Pr}_{68}\text{Cu}_{32}$ are cooled from 1000 °C to room temperature, a series of phase transformation will occur, which are registered as exothermal peaks on DSC curves. The DSC curves of a non-Pr-Cu added magnet sample, a 7.5 wt% Pr-Cu-added magnet sample and a non-La-containing Neo magnet sample for comparison are shown in Fig. 1. Two peaks/bumps in the heating curves correspond to the Curie temperature of 2:14:1 phase (lower temperature) and eutectic temperature of RE-rich phase (higher temperature), respectively. The DSC curves during cooling show the transformation

of the eutectic RE-rich phase and another transformation which corresponds to the Curie temperature of α -Fe (or α -FeCo). These results indicate that free-Fe is first formed and then the 2:14:1 phase when the DSC samples are slowly cooled at a rate of 20°C/min. It is deduced from relative intensities of the exotherms that only a small amount of α -Fe is formed in the non-La-containing Neo magnet (see Fig1c), while a considerable amount of α -Fe is formed in the NdLa magnets (Fig. 1a and b). For the sample with 7.5 wt% Pr-Cu addition, there are two transformation peaks near 850°C, which appear to be the Curie temperatures of different FeCo-based phases. These results confirm that the stability of NdLa 2:14:1 phase is much lower than that of Nd 2:14:1 phase. Moreover, the eutectic temperature of RE-rich phase in the NdLa magnets is lower than that in the non-La-containing Neo magnet. The addition of Pr-Cu results in a further decrease of the eutectic temperature from 490 to 448°C. It is known that the eutectic temperature of $\text{Pr}_{68}\text{Cu}_{32}$ is about 442°C (also with theas 472°C). While sintering and annealing, the Pr-Cu alloy diffuses to the GB areas and combines with the RE-rich phase to form a new RE-rich phase with a lower eutectic temperature.

It was well known that the coercivity H_{cj} of as-sintered Neo magnets (Nd-Fe-B) is developed through two-step annealing near 900°C and 600°C, respectively. We hypothesize that each newly formed phase may require a dedicated temperature to be uniformly distributed on the GB and that annealing at higher temperature may hinder the formation of these lower-temperature phases. To find out the optimum combination of heat treatment temperatures, we designed ten annealing schedules (T1 to T10) based on the transformation temperatures on the DSC curves in Fig 1, and Neo magnets' two-step annealing near 900°C and 600°C. Details of these schedules are shown in Table II. Six magnets (S1 to S6) were made using six different combinations of these heat treatment schedules. Details of these heat treatment combinations and the H_{cj} of the magnets

made with these combinations are listed in Table III. Note that the H_{cj} was measured on the same magnet in between each heat treatment. For example, sample S5 exhibits $H_{cj} = 1.5$ kOe after sintering, and $H_{cj} = 5.4$ kOe after applying heat treatment T4 (580 °C for 2 hrs); H_{cj} was further improved to 6.8 kOe after additional heat treatment T6 (500 °C for 3 hrs). More sequential heat treatments T8 (480 °C for 4 hrs) and T9 (460 °C for 24 hrs) further improved H_{cj} to 7.6 kOe and 9.0 kOe, respectively. At that stage, the magnet S5 reached its peak properties, and any subsequent heat treatments did not further improve H_{cj} . Figure 2 depicts the evolution of H_{cj} as a function of these annealing steps. The highest H_{cj} was achieved by the sample S5, which went through the heat treatment combination of T4 + T6 + T8 + T9. Annealing at a temperature close to 900 °C, i.e., one of the typical two step post-sinter annealing temperatures for Neo magnet, did not improve H_{cj} as effective as annealing at lower temperatures.

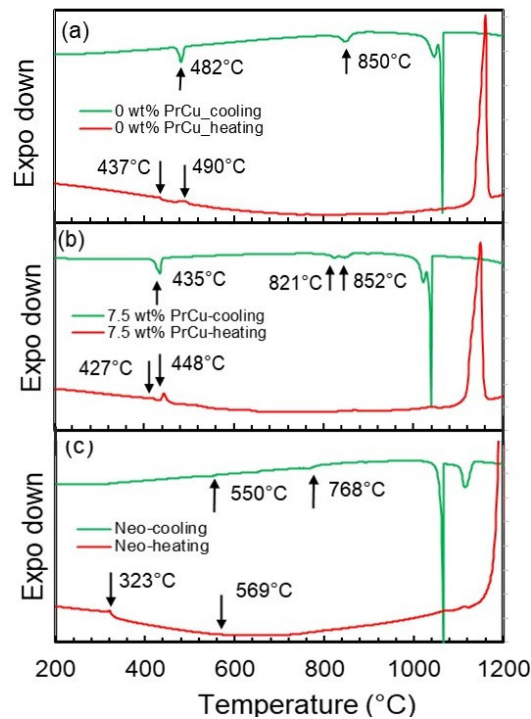


Figure 1. DSC traces of as-sintered magnet without Pr-Cu addition (a), as-sintered magnet with 7.5 wt% Pr-Cu addition (b) and non-La-containing Neo magnet (c)

Table II. Post-sinter annealing schedule and H_{cj} of the treated samples. Skipped annealing steps were marked with “\”. Note that samples S1 to S6 were cut from the same sintered block.

ID	Temperature (°C)	Time (h)	H_{cj} (kOe)					
			S1	S2	S3	S4	S5	S6
T0	1080	1.5	1.5	1.5	1.5	1.5	1.5	1.5
T1	900	0.5	1.5	\	\	\	\	\
T2	820	2	\	2.0	\	\	\	\
T3	580	1	\	\	4.4	\	\	\
T4	580	2	3.8	\	\	\	5.4	4.8
T5	520	3	\	\	\	\	\	5.6
T6	500	3	\	\	\	\	6.8	\
T7	500	2	\	3.8	5.0	3.9	\	\
T8	480	4	4.7	5.2	6.5	5.4	7.6	6.2
T9	460	24	6.6	7.6	8.4	7.9	9.0	7.1
T10	440	24	6.8	6.7	7.1	7.9	8.8	\

Sample S5 was subjected to six different heat treatment combinations, labeled as C0, C1, ..., to C5. The demagnetization curves of S5 subjected to each heat treatment combination are shown in Figure 3 and summarized in Table III. The results show that M_s and B_r are largely constant, not affected by the variation in annealing schedules, but H_{cj} and $(BH)_{max}$ increase with each subsequent annealing step, reaching 9 kOe and 32.4 MGOe after the heat treatment combination C4. There was slight decrease of H_{cj} and $(BH)_{max}$ after the combination C5. This result is comparable to the values of 6.2 kOe and 35.5 MGOe reported by Fan et al.¹⁰ and superior to the values of 3.8 kOe and 24 MGOe reported by Jin et al.¹²

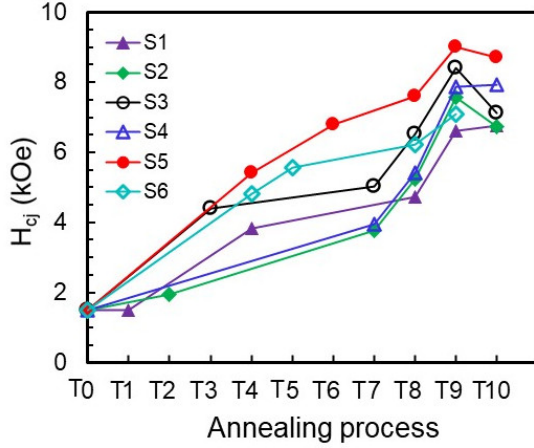


Figure 2. Evolution of H_{cj} as a function of annealing schedules

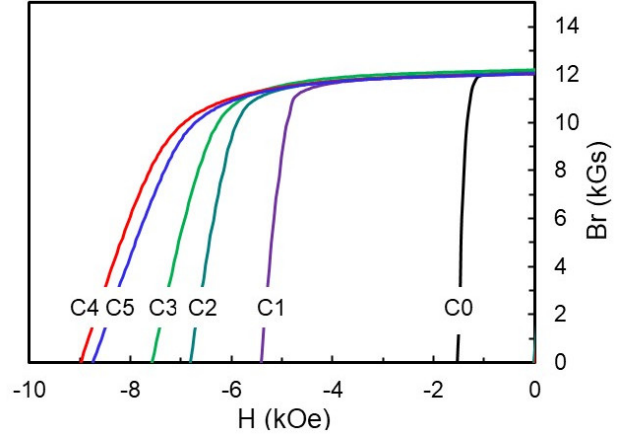


Figure 3. Demagnetization curves of Sample 5 at different annealing steps

Table III. Evolution of magnetic properties of Sample 5 with multi-step annealing

Annealing schedule	T0 (C0)	T0+T4 (C1)	T0+T4+T6 (C2)	T0+T4+T6+T8 (C3)	T0+T4+T6+T8+T9 (C4)	T0+T4+T6+T8+T9+T10 (C5)
M_s (kGs)	12.4	12.3	12.3	12.4	12.2	12.2
B_r (kGs)	12.1	12.1	12.1	12.2	12.0	12.0
H_{cj} (kOe)	1.5	5.4	6.8	7.6	9.0	8.8
$(BH)_{max}$ (MGOe)	12.6	31.2	32.2	32.8	32.4	32.1

To elucidate the role of Pr-Cu in microstructural development, magnets with and without Pr-Cu GB modifier were annealed using the same heat treatment schedule (C4). The H_{cj} of the magnets with (S5) and without Pr-Cu additions are 9 kOe and 4.8 kOe, respectively (Fig. 4). Although adding non-magnetic Pr-Cu alloy decreases the magnetization, the Pr-Cu-added magnet still achieved a much higher $(BH)_{max}$ due to the much-improved H_{cj} .

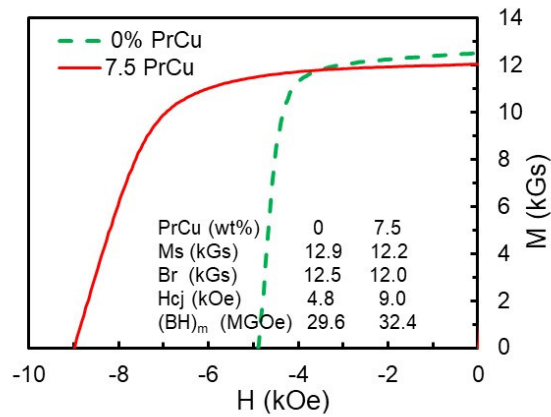


Figure 4. Demagnetization curves of magnets with and without adding 7.5 wt% Pr-Cu alloy. Both magnets were annealed using the schedule C4 shown in Table 3.

Microstructures of the sample 5 magnets after these annealing treatments were studied with SEM. The microstructures did not exhibit any obvious change as the results of these annealing treatments. Fig. 5 shows the BSE images of sample 5 magnet annealed at annealing step C0 and C4.

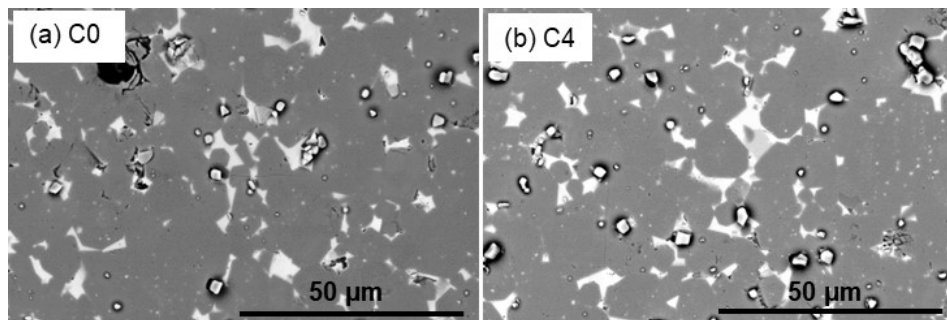


Figure 5. SEM BSE images of sample 5 magnets annealed at annealing step C0 and C4.

Elemental mapping of the as-sintered (C0) magnet (Fig 6a) and the fully annealed (i. e. C4) magnet (Fig. 6b) show that the REE, Cu, and Ga, are concentrated at the grain boundaries and triple junctions. The EDS composition analysis (Fig. 7) was used to quantitatively show the variations of element concentration as a function of the annealing steps. The locations of the EDS

analysis include grain core (center areas of grains) and GB and triple junction areas (GB&TJ). Figure 7 shows that annealing from C1 to C4 at lower temperatures results in higher Cu and Nd and lower La and Ga concentrations at the GB&TJ areas. Further annealing in C5 results in decrease of Cu and increase of Fe. Elements at the grain core do not show any significant changes with various annealing steps. These results confirm that the post-sinter annealing primarily changes the compositions at the GB&TJ areas.

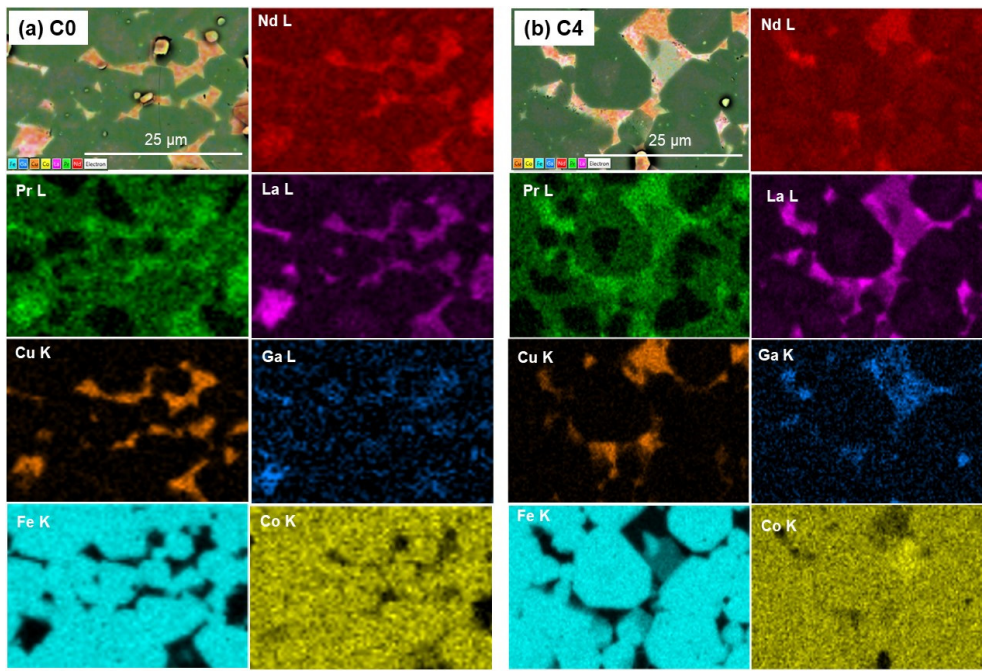


Figure 6. Composition mapping of as-sintered magnet (a) and annealed magnet S5 (b).

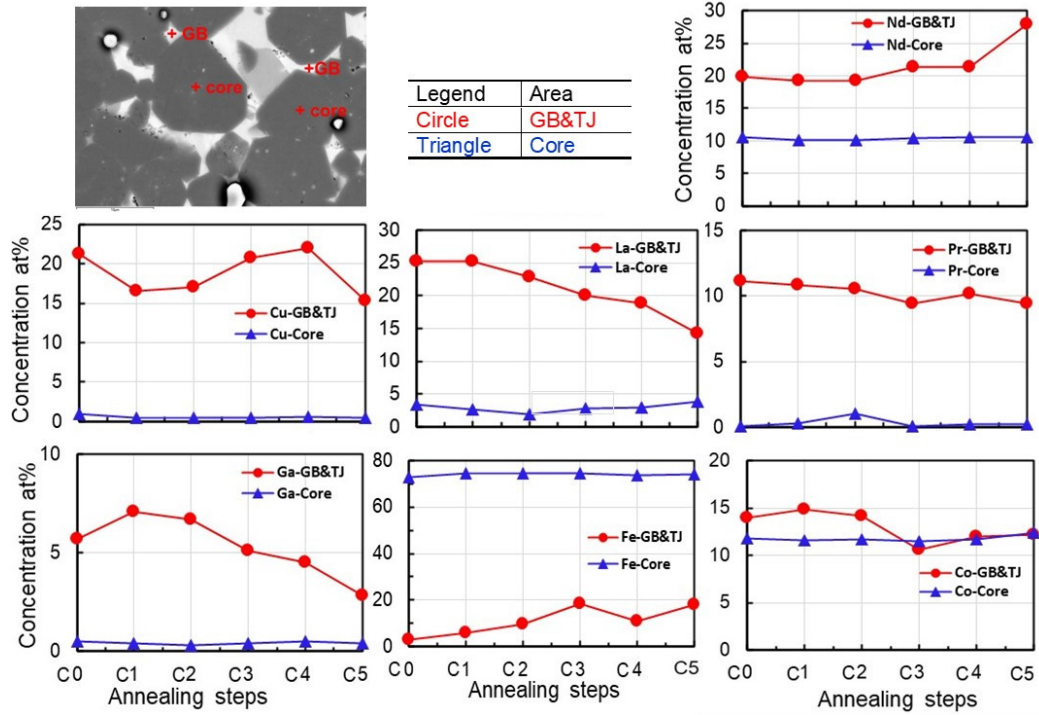


Figure 7. Composition variations with annealing steps at grain boundary & trip junction (denoted as GB&TJ), and grain core areas. An SEM BSE image illustrates the spectrum spots analyzed by EDS in these areas. A table lists legends and their corresponding areas in figures.

IV. DISCUSSION

The coercivity of Neo magnets depends on their intrinsic properties such as anisotropy field and extrinsic properties such as microstructures. Grain size, shape/morphology, and boundary phase/chemistry contribute to magnet's coercivity. The post-sinter annealing mainly impacts the distribution of GB phase and its chemical concentration.

When the samples were sintered at 1080 °C, the RE-rich phase and Pr-Cu alloy melted and distributed at GB&TJ areas. They are diffused along the GB and TJ regions with composition changes when the magnet is annealed at lower temperatures. Non-La-containing Neo sintered magnets obtain a high H_{cj} through two step annealing near 900°C and 600°C, respectively^{22,26,27}.

There exist stress and defects on the surface of grains, and chemical inhomogeneity at GB and TJ regions in as-sintered magnets. Liu's studies²⁸ revealed that the stress and interfacial energy at the Nd-rich/Nd₂Fe₁₄B interface are reduced after two-step annealing, and the interface becomes relatively flat and smooth, accompanying with a transformation of the crystal structure of Nd-rich phase from dhcp to fcc. A smooth and stress-relieved fcc-Nd-rich/ Nd₂Fe₁₄B interface reduces the probability of reversed domain nucleation and thus enhances H_{cj}. Moreover, studies have confirmed that the two-step annealing promotes the formation of continuous Nd-rich GB phase^{29, 30}. The generally accepted theory cited in literature is the first step in the process of annealing near 900°C is to mainly eliminate the defects, release the stress and homogenize the interface concentrations, while the second step of annealing near 600°C is to promote the formation of continuous GB phase and change the chemistry and distribution of the GB phase.

We have found that the La-substituted Neo magnets doped with Pr-Cu GB modifier, annealed near 900°C before lower temperature annealing did not improve properties. Samples S1 and S2 were first annealed at 900 and 820 °C, respectively, then were annealed at lower temperatures (see Table II). The resulting H_{cj} were only 6.8 and 6.7 kOe, respectively. In comparison, sample S5 that skipped the high temperature annealing achieved a H_{cj} of 9 kOe. It is shown in Fig 1a, b that the substitution of La for Nd not only changes the temperatures of phase transformation, but also diminishes the stability of (NdLa)₂Fe₁₄B phase. Especially after addition of 7.5 wt% Pr-Cu, two FeCo-based phases were formed when the sample was cooled below 900 °C (see Fig. 1b). In this case, although annealing near 900 °C helps to release the stress and homogenize the interface concentrations, which is positive to achieve a higher H_{cj}, it also promotes the formation of more FeCo-based phases. Based on these results, we find that annealing at 900 °C is not beneficial to improve the H_{cj} of the La-substituted Neo magnets.

Annealing at lower temperatures changes the chemistry and distribution of the GB phases. A desired microstructure and local chemistry can be achieved if the annealing dwelling time is long enough at a lower temperature. The annealing at 580 °C mainly impacts the re-distribution of RE-rich and Pr-Cu phases, while the annealing at 480 and 460°C promotes the redistribution of Pr-Cu in the GB. Further annealing at 440 °C for 24 h did not improve H_{cj} . Despite being a relatively low temperature, annealing at 440 °C caused noticeable increase of (Fe, Nd) content, and decrease of (La, Cu, Ga) contents in the GB & TJ regions. It is not clear what phases were forming due to the long annealing at 440 °C, but the resultant increase in Fe content may favor more magnetically soft behavior.

While the addition of GB modifier Pr-Cu alloy improves coercivity, it reduces saturation magnetization and softens the squareness of demagnetization curves, as shown in Fig.4. The amount of the Pr-Cu powder added to the master alloy powder is relatively small (7.5 wt% Pr-Cu vs 92.5 wt% master alloy powder). When the particle size of both powders is the same, the amount is not sufficient for even distribution in between all LaNd-FeCo-B particles. Consequently, Pr-Cu may not be evenly distributed in between all grain at the boundary and triple junction after sintering and post-sinter annealing. The region with less GB phases may experience early domain reversal, causing the overall demagnetization curve to be less square. How to uniformly distribute the GB modifier at the desired location with the desired amount is the challenge for Nd-lean magnet to achieve a H_{cj} beyond 10 kOe.

V. CONCLUSIONS

We have mapped out the magnetic properties of (Nd,La)-based magnets over a wide-range of multi-step annealing at various temperatures and dwelling times. We find that annealing at

higher temperatures (820 or 900 °C) has negative effects on developing H_{cj} of the $(Nd_{0.75}La_{0.25})_{2.6}Fe_{11.9}Co_2Ga_{0.1}B$ magnet doped with 7.5wt% Pr-Cu GB modifier. An optimal annealing schedule was developed that involves annealing at 580 °C, which is higher than the eutectic temperature ($\sim 450^\circ C$) of the RE-rich phase in the NdLa-FeCo-B magnet, followed by annealing at 500, 480, and 460 °C, all of which are near the eutectic temperature of the RE-rich phase. Prolonged annealing at 480 and 460 °C helps Nd, Pr, and Cu-rich phases to distribute at GB&TJ phase regions. Further annealing at 440°C for 24 h led to a slight Cu decrease and Fe increase at GB&TJ phase regions, thus decreasing H_{cj} . The fully annealed magnet reached a H_{cj} of 9 kOe and $(BH)_{max}$ of 32.4 MGOe.

ACKNOWLEDGMENT

This work is supported by the Critical Materials Innovation (CMI) Hub, funded by the U.S. Department of Energy (DOE), Office of Energy Efficiency and Renewable Energy, Advanced Materials and Manufacturing Technologies Office (AMMTO). The work was performed in Ames National Laboratory, operated for the U.S. Department of Energy by Iowa State University of Science and Technology under Contract No. DE-AC02-07CH11358.

Declaration of interests

On behalf of all authors, the corresponding author states that there is no conflict of interest in this paper.

Reference

- ¹ M. Sagawa, S. Fujimura, N. Togawa, H. Yamamoto, Y. Matsuura, New material for permanent magnets on a base of Nd and Fe (invited), *J. Appl. Phys.* 55 (1984) 2083. <https://doi.org/10.1063/1.333572>.
- ² J.M.D. Coey, Perspective and Prospects for Rare Earth Permanent Magnets, *Engineering*. 6 (2020) 119–131. <https://doi.org/10.1016/j.eng.2018.11.034>.
- ³ Cui, J., Ormerod, J., Parker, D., Ott, R., Palasyuk, A., Mccall, S., Paranthaman, M.P., Kesler, M.S., McGuire, M.A., Nlebedim, I.C. and Pan, C., 2022. Manufacturing processes for permanent magnets: Part I—sintering and casting. *Jom*, 74(4), pp.1279-1295.
- ⁴ United States. Bureau of Mines. Mineral Facts and Problems: 1985 Edition, report, 1985; Washington D.C.
- ⁵ J. F. Herbst, "R2Fe14B materials: Intrinsic properties and technological aspects," *Reviews of Modern Physics*, vol. 63, 1991.
- ⁶ Z. Li, W. Liu, S. Zha, Y. Li, Y. Wang, D. Zhang, M. Yue, J. Zhang, Effects of lanthanum substitution on microstructures and intrinsic magnetic properties of Nd-Fe-B alloy, *J. Rare Earths*. 33 (2015) 961–964. [https://doi.org/10.1016/S1002-0721\(14\)60512-3](https://doi.org/10.1016/S1002-0721(14)60512-3).
- ⁷ X.B. Liu, Z. Altounian, M. Huang, Q. Zhang, J.P. Liu, The partitioning of α and γ in Nd-Fe-B magnets: A first-principles study, *J. Alloys Compd.* 549 (2013) 366–369. <https://doi.org/10.1016/j.jallcom.2012.10.056>.
- ⁸ W. Tang, S. Zhou, R. Wang, Preparation and microstructure of La-containing R-Fe-B permanent magnets, *J. Appl. Phys.* 65 (1989) 3142–3145. <https://doi.org/10.1063/1.342711>.
- ⁹ X. Li, Z. Lu, Q. Yao, Q. Wei, J. Wang, Y. Du, L. Li, Q. Long, H. Zhou, G. Rao, Thermal stability of high-temperature compound La₂Fe₁₄B and magnetic properties of Nd-La-Fe-B alloys, *J. Alloys Compd.* 859 (2021). <https://doi.org/10.1016/j.jallcom.2020.157780>.
- ¹⁰ X. Fan, G. Ding, K. Chen, S. Guo, C. You, R. Chen, D. Lee, A. Yan, Whole process metallurgical behavior of the high-abundance rare-earth elements LRE (La, Ce and Y) and the magnetic performance of Nd_{0.75}LRE_{0.25}-Fe-B sintered magnets, *Acta Mater.* 154 (2018) 343–354. <https://doi.org/10.1016/j.actamat.2018.05.046>.
- ¹¹ X.F. Liao, L.Z. Zhao, J.S. Zhang, X.C. Zhong, D.L. Jiao, Z.W. Liu, Enhanced formation of 2:14:1 phase in La-based rare earth-iron-boron permanent magnetic alloys by Nd substitution, *J. Magn. Mater.* 464 (2018) 31–35. <https://doi.org/10.1016/j.jmmm.2018.05.041>.

-
- ¹² J. Jin, Z. Wang, G. Bai, B. Peng, Y. Liu, M. Yan, Microstructure and magnetic properties of core-shell Nd-La-Fe-B sintered magnets, *J. Alloys Compd.* 749 (2018) 580–585. <https://doi.org/10.1016/j.jallcom.2018.03.291>.
- ¹³ M. Zhu, W. Li, J. Wang, L. Zheng, Y. Li, K. Zhang, H. Feng, T. Liu, Influence of Ce content on the rectangularity of demagnetization curves and magnetic properties of Re-Fe-B magnets sintered by double main phase alloy method, *IEEE Trans. Magn.* 50 (2014). <https://doi.org/10.1109/TMAG.2013.2278018>.
- ¹⁴ E. Niu, Z.A. Chen, G.A. Chen, Y.G. Zhao, J. Zhang, X.L. Rao, B.P. Hu, Z.X. Wang, Achievement of high coercivity in sintered R-Fe-B magnets based on misch-metal by dual alloy method, *J. Appl. Phys.* 115 (2014). <https://doi.org/10.1063/1.4869202>.
- ¹⁵ H. Chen, W. Liu, Z. Guo, T. Yang, H. Wu, Y. Qin, Y. Li, H. Zhang, M. Yue, Coercivity enhancement of Nd-La-Ce-Fe-B sintered magnets: Synergistic effects of grain boundary regulation and chemical heterogeneity, *Acta Mater.* 235 (2022). <https://doi.org/10.1016/j.actamat.2022.118102>.
- ¹⁶ J. Jin, T. Ma, Y. Zhang, G. Bai, M. Yan, Chemically Inhomogeneous RE-Fe-B Permanent Magnets with High Figure of Merit: Solution to Global Rare Earth Criticality, *Sci. Rep.* 6 (2016). <https://doi.org/10.1038/srep32200>.
- ¹⁷ H. Zeng, Z. Liu, W. Li, J. Zhang, L. Zhao, X. Zhong, H. Yu, B. Guo, Significantly enhancing the coercivity of NdFeB magnets by ternary Pr-Al-Cu alloys diffusion and understanding the elements diffusion behavior, *J. Magn. Magn. Mater.* 471 (2019) 97–104. <https://doi.org/10.1016/j.jmmm.2018.09.080>.
- ¹⁸ T.H. Kim, S.R. Lee, S.J. Yun, S.H. Lim, H.J. Kim, M.W. Lee, T.S. Jang, Anisotropic diffusion mechanism in grain boundary diffusion processed Nd-Fe-B sintered magnet, *Acta Mater.* 112 (2016) 59–66. <https://doi.org/10.1016/j.actamat.2016.04.019>.
- ¹⁹ F. Wan, Y. Zhang, J. Han, S. Liu, T. Liu, L. Zhou, J. Fu, D. Zhou, X. Zhang, J. Yang, Y. Yang, J. Chen, Z. Deng, Coercivity enhancement in Dy-free Nd-Fe-B sintered magnets by using Pr-Cu alloy, *J. Appl. Phys.* 115 (2014). <https://doi.org/10.1063/1.4879898>.
- ²⁰ M. Tang, X. Bao, Y. Zhou, K. Lu, J. Li, X. Gao, Microstructure and annealing effects of NdFeB sintered magnets with Pr-Cu boundary addition, *J. Magn. Magn. Mater.* 505 (2020). <https://doi.org/10.1016/j.jmmm.2020.166749>.
- ²¹ K. Lu, X. Bao, M. Tang, L. Sun, J. Li, X. Gao, Influence of annealing on microstructural and magnetic properties of Nd-Fe-B magnets by grain boundary diffusion with Pr-Cu and Dy-Cu alloys, *J. Magn. Magn. Mater.* 441 (2017) 517–522. <https://doi.org/10.1016/j.jmmm.2017.03.049>.
- ²² WF Li, T. Ohkubo, K. Hono, Effect of post-sinter annealing on the coercivity and microstructure of Nd-Fe-B permanent magnets, *Acta Mater.* 57 (2009) 1337–1346. <https://doi.org/10.1016/j.actamat.2008.11.019>.
- ²³ F. Vial, F. Joly, E. Nevalainen, M. Sagawa, K. Hiraga, K.T. Park, Improvement of coercivity of sintered NdFeB permanent magnets by heat treatment, 2002.

-
- ²⁴ Y. Zhang, T. Ma, M. Yan, J. Jin, B. Wu, B. Peng, Y. Liu, M. Yue, C. Liu, Post-sinter annealing influences on coercivity of multi-main-phase Nd-Ce-Fe-B magnets, *Acta Mater.* 146 (2018) 97–105. <https://doi.org/10.1016/j.actamat.2017.12.027>.
- ²⁵ W. Tang, G. Ouyang, J. Wang, H. Dasari, M. J. Kramer, I. E. Anderson, and J. Cui, Development of Dy-free Nd-Fe-B-based sintered magnet through grain boundary engineering using Pr-Cu alloys, *IEEE Trans. Magn.* 59 (2023) 2100603. <https://doi.org/10.1109/TMAG.2023.3282430>.
- ²⁶ R. Mishra, J. Chen, G. Thoms, Effect of annealing on the microstructure of sintered Nd-Fe-B magnets, *J. Appl. Phys.* 59 (1986) 2244-2246. <https://doi.org/10.1063/1.336366>
- ²⁷ T. Kim, S. Lee, S. Namkung, T. Jang, A study on the Nd-rich phase evolution in the Nd-Fe-B sintered magnet and its mechanism during post-sintering annealing, *J. Alloys Compd.* 537(2012) 261-268. <https://doi.org/10.1016/j.jallcom.2012.05.075>.
- ²⁸ Qiongzen Liu, Fang Xu, Jing Wang, Xianping Dong, Lanting Zhang and Junyou Yang, An investigation of the microstructure in the grain boundary region of Nd-Fe-B sintered magnet during post-sintering annealing, *Scripta Materialia* 68(2013) 687-690, <http://dx.doi.org/10.1016/j.scriptamat.2013.01.019>
- ²⁹ G H Yan, R J Chen, Y Ding, S Guo, Don Lee and A R Yan, “The preparation of sintered NdFeB magnet with high-coercivity and high temperature stability”, *Journal of Physics: Conference Series* 266(2011)012052, doi:10.1088/1742-6596/266/1/012052.
- ³⁰ Qing zhou, We Li, Yuan Hong, Lizhong Zhao, Xichun Zhong, Hongya YU, Lili Huang, Zhongwu Liu, Microstructure improvement related coercivity enhancement for sintered NdFeB magnets after optimized additional heat treatment. *Journal of Rare Earths*, 36 (2018) 379-384, <https://doi.org/10.1016/j.jre.2017.11.007>.